

Investigation of newly developed added damping and stiffness device with low yield strength steel

SHIH Ming-hsiang^{†1}, SUNG Wen-pei^{†2}, GO Cheer-germ³

⁽¹⁾Department of Construction Engineering, National Kaoshiang First University of Science and Technology, Taiwan 824, China)

⁽²⁾Department of Landscape Design and Management, National Chin-Yi Institute of Technology, Taiwan 41111, China)

⁽³⁾Department of Civil Engineering, National Chung Hsing University, Taiwan 40227, China)

[†]E-mail: mhshih@cems.nkfust.edu.tw; sung809@chinyi.ncit.edu.tw

Received Mar. 15, 2003; revision accepted Aug. 25, 2003

Abstract: Energy dissipators, isolated-resistant and specific structural forms for earthquake resistance are popular topics in the research to improve shock-resistance. In this work, experimental methods were used to investigate the property of low yield strength steel. Carbon content in LYS material is lower than that in other steels; the ultimate stress is three times the yield stress. The ultimate elongation rate is about 62% and the ductility is 2–3 times that of A36 steel. In order to overcome some defects of ordinary use metallic dampers, the mechanical characteristic of low yield strength steel is used to develop added damping and stiffness for rhombic steel plate absorber. Test of the energy dissipation behavior for this newly developed device indicated that LYS could stably dissipate or absorb the input energy of earthquake. Then, the analytical model for the hysteretic behavior of this new device is proposed. Comparison of experimental data and numerical simulation results showed that this analytical model is suitable for simulating the hysteretic energy behavior of this new device.

Key words: Seismic shock absorbance elements, Capability of seismic resistance, Hysteretic behavior of rhombic steel plate, Nonlinear analytical model

Document code: A

CLC number: TU311.3

INTRODUCTION

This research focused on using the mechanical properties of low yield strength steel (LYS) to develop a new device for added damping and stiffness and seismic resistance of rhombic low yield strength steel plate. The mechanical properties of LYS and the effect of this newly developed device were investigated by experimental method. Expectedly, this new device can take advantage of plastic energy absorbability to absorb and dissipate the energy of earthquake stably and ensure the safety of the main structure. An analytical model is proposed for analyzing the hysteresis loop and mechanical characteristics of this device.

The traditional concept of resisting earthquake-induced forces is to increase the intensity, stiffness and ductility of structure as the design criteria. A general principle of ductile design is that the ductility of a structure can be enhanced after yielding of the main structure to avoid collapse of the structure. Simultaneously, there are some flaws in this design concept: (1) the main frame of the structure will not be destroyed, and its emplaced equipment will be damaged and thus cause the function of livelihood to be ruined; (2) the complication of ductility logic design. The actual ductile capability of each member cannot assuredly match the design hypothesis; (3) the secondary moment induced by large deformation of earth-

quake causes the destruction of the structure. New structural control theory based techniques are important parts of recent research outlines. The development of passive energy absorber is the most suitable approach for improving resistance to earthquake-induced forces (Wada *et al.*, 1992; Iwata *et al.*, 1995; Constantinou *et al.*, 1998; Tsai and Le, 1993). The basic principle of the passive energy absorber is to use the damper, a steel passive energy dissipation, steel device for providing seismic resistance by absorbing and dissipating the major part of earthquake energy. Often used steel devices for earthquake resistance are the X (Whitaker *et al.*, 1989; Xia and Hanson, 1992), and triangular (Tsai, 1992; Tsai *et al.*, 1993) type of steel plate device for added damping and stiffness, matched with bracing to install in frame. The effect of energy dissipation is very good. Nevertheless, the following problems still exist in these two types of steel earthquake resistance devices.

1. The top and bottom of X type steel plate use bolts to fix the bottom of the beam to the bracing. Under loading and after deformation, the steel plate's taking the axial force affects its mechanical behavior.

2. The triangular steel plate type is used to bypass the axial force problem. However, the welding bond is used to combine the triangular steel plate and the bottom plate and then connect them to the bottom of the beam. The qualities of welding bond affect the effect of energy dissipation. Additionally, economy is not consistent utility in this type.

Reciprocal action causes local fracture on X and triangular type of steel plate (Tsai and Chou, 1996). To improve the earthquake resistance capability, and the effect of energy dissipation, low yield strength steel was used to develop the energy

dissipator-high seismic resistance rhombic low yield strength steel. Experimental method was used to investigate the mechanical properties of low yield strength steel and the earthquake resistance capability of this newly developed device. Additionally, a reasonable mathematical model, combined with the mechanical properties of LYS, is proposed to analyze the hysteretic behavior of this device, based on Wen's model and Bouc-Wen differential model (Bouc, 1967; Wen, 1976).

EXAMINATION OF LOW YIELD STRENGTH STEEL

To investigate the supremacy of resistance earthquake and the basic mechanical properties of low yield strength steel (LYS), experimental method was used to test the material produced by the China Steel Corporation (Chang and Wang, 1997) and compare it with the often-used A36 steel.

Test method

LYS samples with thickness of 16 mm and 5 mm were used for the tensile test. The LYS test piece of 16 mm used an oil jacket capable of 200 tons effective pull force. An elongation gauge was used to measure the relative elongation for calculation of the strain value. The test piece of 5 mm used an oil jacket capable of 100 tons effective pull force. The strain gauge and elongation gauge should coordinate with each other to obtain the strain value. The specifications of equipment for the material test are listed in Table 1.

Experimental results

Small strain theory and real stress-strain theory to calculate the Young's modulus, yielding stress,

Table 1 Specification of equipment for material test

Equipment	Type	Capacity and accuracy
200 Tn Universal Test Mach.	FORNEY LT-0950	100 kg
10 Tn Universal Test Mach.	SHIMADZU AG-10TG	1 kg
Elongation Gauge	MTS Model634.28F-54	0.01 mm (relative to strain=0.0001)
Strain Amp.	KYOWA DPM-700B	0.001 V
Strain Gauge	KYOWA 120 Ω	0.00001

ultimate stress and rate of the ultimate elongations from the measured experimental results from the material test.

1. Small strain theory

According to the definition of the small strain theorem, strain is the proportion of measured elongation to original length. Stress is the measured loading divided by the original area. The equations are shown as follows:

$$\epsilon = \frac{\Delta L}{L_0} \tag{1}$$

$$\sigma = \frac{F}{A_0} \tag{2}$$

Where L_0 is original length; A_0 is original area; F is measured loading from test.

2. Real stress-strain theory

According to the definition of "Mechanics of Materials"(Gere and Timoshenko, 1990) and "Plas-

ticity: Theory and Application" (Mendelson, 1970), the real strain can be defined as follows:

$$\epsilon_t = \ln(1 + \epsilon) \tag{3}$$

Where: ϵ_t is real strain; ϵ is the strain based on the definition of small strain theory.

The real cross section of area and real stress can be obtained by the real strain. The equations are shown as follows:

$$A_t = A_0 [\exp(-2\nu\epsilon_t)] \tag{4}$$

$$\sigma_t = \frac{P}{A_t} = \sigma [\exp(2\nu\epsilon_t)] \tag{5}$$

Where: A_t is real cross section of area; A_0 is original cross section of area; P is loading value; σ_t is real stress; σ is the stress based on small strain theory; ν is Poisson ratio.

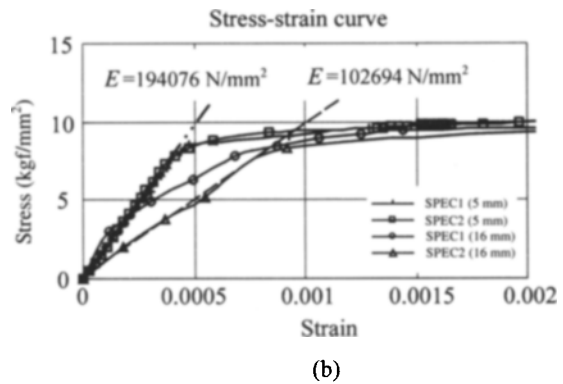
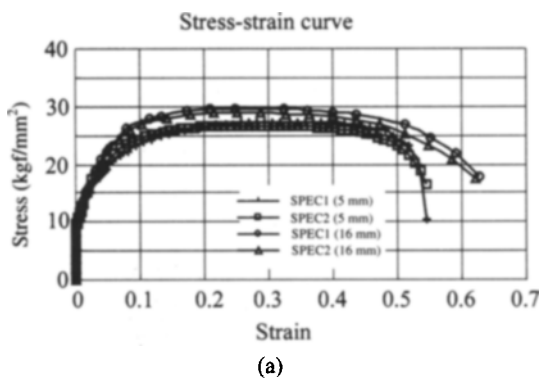


Fig.1 Stress-strain curves of small strain theory
(a) Ultimate strain; (b) Small strain

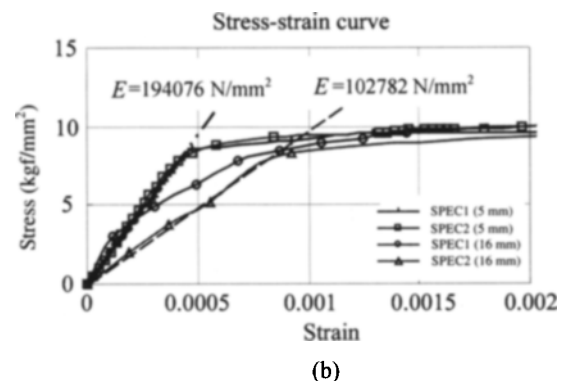
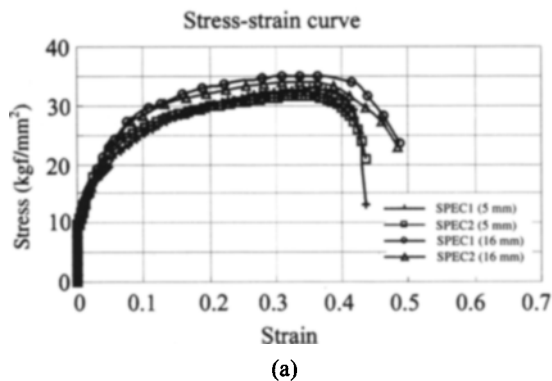


Fig.2 Stress-strain curves of real stress-strain theory
(a) Ultimate strain; (b) Small strain

Table 2 The comparison between LYS-100 and A36

	LYS-100 (5 mm)		LYS-100 (16 mm)		A36*
	Small def.	Real def.	Small def.	Real def.	
Young's modulus (N/mm ²)	194 706	194 706	102 694	102 782	200 000
Yielding stress σ_y (N/mm ²)	100.8	101.0	97.5	97.6	250
Yielding strain ϵ_y	0.00052	0.00052	0.00096	0.00097	0.00125
Ultimate stress σ_u (N/mm ²)	270.3	322.0	292.0	345.0	400
Ultimate strain ϵ_u	0.55	0.44	0.62	0.49	0.3

*Information: "Mechanics of Materials", by Gere and Timoshenko (1990)

Experimental results are shown in Figs.1, 2 and Table 2. Conclusions derived were as following:

(1) The Young's modulus obtained from the test of the 5 mm specimen was 1.88 times that from the test of the 16 mm specimen. The result from the test of the 5 mm specimen was very close to the Young's modulus. Thus, in order to acquire the accuracy of Young's modulus, a strain gauge should be used to measure the strain of the small deformation.

(2) The test result for Young's modulus, using 0.2% offset to obtain the yielding stress was about 10 kgf/mm².

(3) Observation of the curve of small deformation in the tensile test indicated that the yield stage of LYS is less obvious than that of A36 steel.

(4) The LYS ultimate stress is about three times that of the yielding stress. The rate of strain hardening of LYS is actually higher than that of A36 steel.

(5) The LYS ultimate strain is about 62% or 1.5 to 2 times that of A36.

Application of LYS in the design of structures capable of resisting earthquake-induced forces is appropriate for plastic hinge, plastic shear link and other energy dissipation control mechanisms.

SEISMIC RESISTANCE OF RHOMBIC LOW YIELD STRENGTH STEEL AND RECIPROCAL LOADING TEST

The often-used steel devices for earthquake resistance are X and triangular type of steel plate

device for added damping and stiffness. Some problems of active behavior and installation of ADAS device include: the influence of axial force, welding and the phenomena of local fracture (Tsai and Chou, 1996). In order to eliminate the defects of these devices, a new seismic resistance – rhombic low yield strength steel was designed and developed as shown in Fig.3. The base of the carrier is shown in Fig.4. Several advantages of this rhombic seismic resistance device are discussed below.

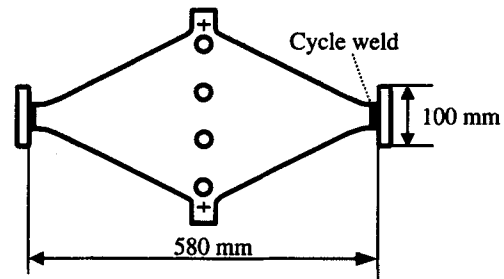


Fig.3 The rhombic steel plate with low yield strength steel for ADAS

(1) The supports type of both ends of rhombic seismic resistance is hinge, so the axial force does not easily affect the rhombic steel plate.

(2) The rhombic steel plate uses symmetry to induce similarly effect at the fixed end. Thus, welded bond need not be used. Therefore, the welding quality cannot influence the energy absorber, and manufacturing cost of this device can be lowered.

(3) The fine property of strain hardening of LYS steel can be used to overcome the local fracture problem at the steel plate of energy dissipator.

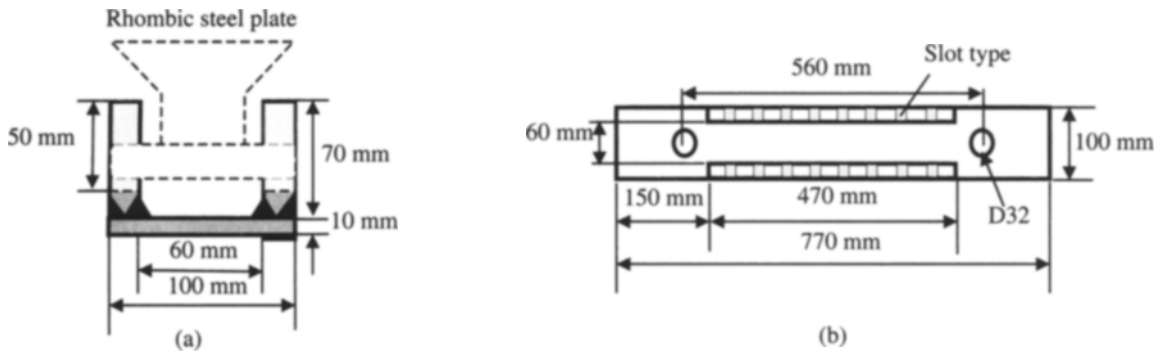


Fig.4 The base of the carrier of newly developed metallic damper
 (a) Side view of the base of the carrier; (b) Front view of the base of the carrier

The advantages of this newly developed energy absorber and the use of the mechanical characteristics of LYS can increase the ductility and energy dissipation capability and decrease the structure reaction to attain the purpose of reducing the earthquake energy. Consequently, the incremental displacement of the reciprocating loading test was used to investigate the basic reaction behavior of seismic resistance of rhombic LYS steel.

Experimental method

To investigate the true effect of energy dissipation of this newly developed device, the method of deflection control was used to reciprocally increase the burden in experimental process. The nominal yielding displacement Δ_{y0} is a basic value, and then the displacements of $0.25\Delta_{y0}$, $0.5\Delta_{y0}$, $0.75\Delta_{y0}$, Δ_{y0} , $1.5\Delta_{y0}$, $2\Delta_{y0}$, $4\Delta_{y0}$, $6\Delta_{y0}$, $8\Delta_{y0}$, $12\Delta_{y0}$, $16\Delta_{y0}$... were used to apply load coming and going until the displacement was up to $40\Delta_{y0}$. The ampli-

tude of $40\Delta_{y0}$ was used for cycle test, and the process of loading is shown in Fig.5. In the process of applied load, the magnitude of applying load, values of displacement and strain of steel plate are recorded by load cell and LVDT. MTS407 was used to measure data on the brake horsepower. The installation of this test is shown in Fig.6.

Test results

Fig.7 shows that the improvement of this detailed item can avoid occurrence of minus moment at

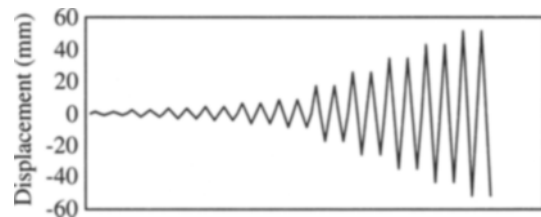


Fig.5 The process of loading

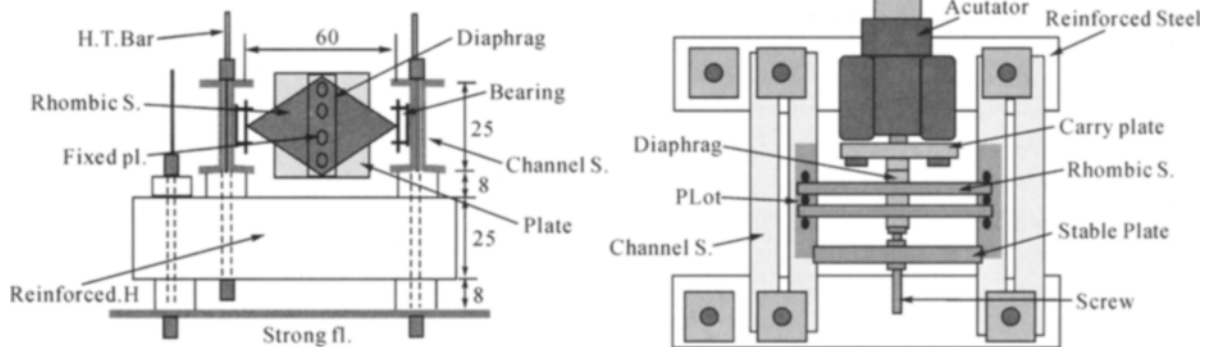


Fig.6 The installation for dynamic test
 (a) Front view; (b) Top view

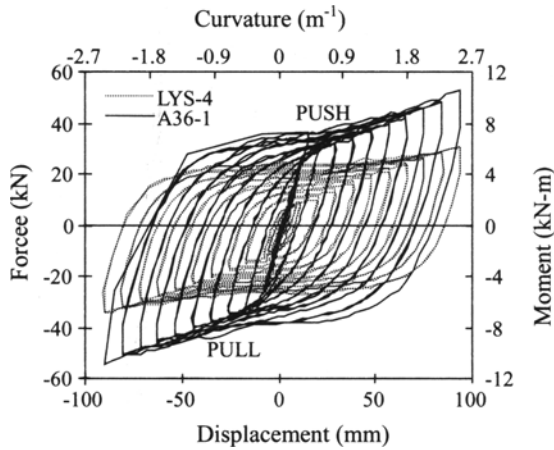


Fig.7 The smoothly hysteresis loop for the history of energy dissipation

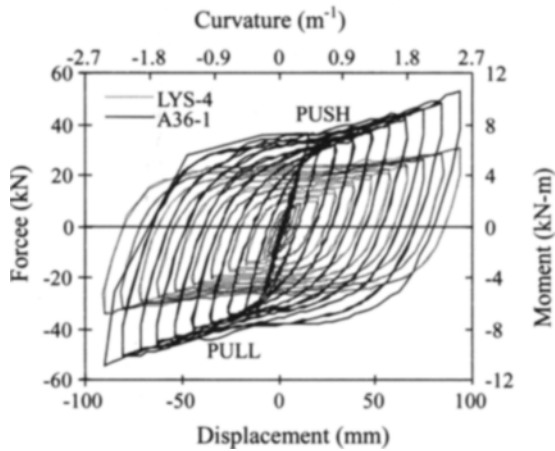


Fig.8 The comparison of hysteresis loop of LYS and A36-ADAS

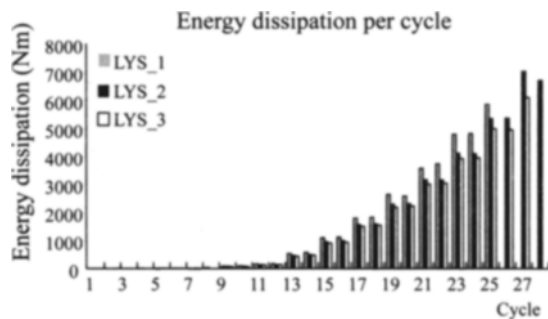


Fig.9 The energy dissipation capability of each rhombic steel plate

the rhombic LYS steel plate. Additionally, in order to compare the difference between LYS and A36 steel application in ADAS device, the rhombic A36

steel was used. Fig.8 shows that the phenomenon of isotropic hardening of LYS is more obvious than A36 steel. Fig.9 indicates the energy dissipation capability of each rhombic steel plate on which each samples loaded the same displacement twice coming and going. It shows that energy dissipation was almost the same for each loop at the same displacement. The energy dissipation capability of this type steel plate was stable. Because of fine strain hardening of LYS, the strain curve at the middle point of the steel plate and the symmetric fixed end were almost the same as shown in Fig.10. Thus, this newly developed type steel plate has advantages of total yield and the same transformation of curvature. It attains the design requirement of added damping and stiffness device.

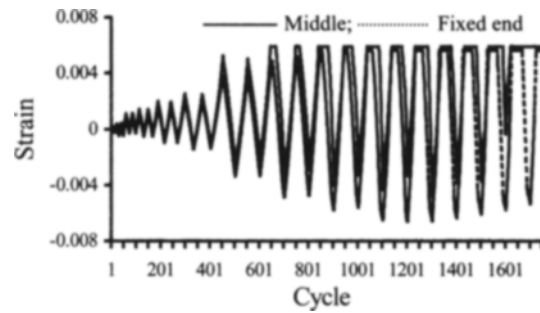


Fig.10 The strain-hardening curve of middle point and fixed end of rhombic steel plate

NUMERICAL SIMULATION MODEL

In order to describe accurately the nonlinear behavior of the LYS-ADAS device under reciprocating loading test, the mechanism of isotropic hardening must be described and added into the mathematical model. From the envelope curve of a maximum connecting line of each cycle under the increasing displacement reciprocating loading test, the hardening behavior of the bounding surface of LYS-ADAS approaches the transformation of double line, shown in Fig.11. Consequently, the change rule of isotropic hardening of LYS-ADAS can be assumed to be as follows:

$$\Delta_y = \begin{cases} \Delta_{y0}, & \text{if } \Delta_{\max} \leq \Delta_{y0} \\ \Delta_{y0} + \mu(\Delta_{\max} - \Delta_{y0}), & \text{if } \Delta_{\max} \geq \Delta_{y0} \end{cases} \quad (6)$$

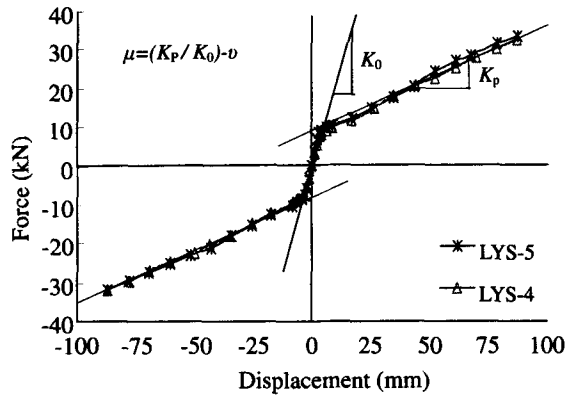


Fig.11 The envelope curve of a maximum connecting line

Where: Δ_{y0} is nominal yielding displacement; Δ_{max} is absolute value of the maximum displacement in the loading history; μ is the difference between the rate of function of double linear hardening at the second line, defined in this paper, and rate of inclination of initial line and rate of kinematic transformation v ; v is stiffness rate before and after yielding.

From the investigation of the influence of the summation of α , β and γ vs. intensity and stiffness (Tanaka and Sasaki, 2000), α is decided by the elastic stiffness of the member under loading; the yielding displacement, that is radius of yielding surface, is decided by the ratio of α and the summation of β and γ , defined as follows:

$$K_e = K_0 \cdot \alpha \tag{7}$$

$$\Delta_y = \left(\frac{\alpha}{\beta + \gamma} \right)^{1/n} \tag{8}$$

Where, K_e is the initial stiffness simulated by Wen's Model; K_0 is the system initial stiffness; α , β , γ and n are the parameters controlling the transformed hysteresis loop.

The experimental data showed that the elastic stiffness of ADAS remained briefly about a constant. Consequently, the α should keep constant in the history of deformation. The yielding displacement trace follows the maximum displacement to increase, thus, the summation of β and γ should be changed to decrease following the increase of the maximum displacement. Moreover, the new pa-

rameter η is defined as the multiplier of β and γ . Consequently, the proposed equation of modified Wen's model can be defined as follows:

$$\dot{q} = \alpha \dot{x} - \eta \left(\beta |\dot{x}| |q|^{n-1} + \gamma \dot{x} |q|^n \right) \tag{9}$$

$$\eta = \left(\frac{\Delta_y}{\Delta_{y0}} \right)^{-n} \tag{10}$$

Where: Δ_y is the present yielding displacement of ADAS, shown in Eq.(6); Δ_{y0} is the nominal yielding displacement; η is between 0 and 1 according to the transformation of deformation history and it is decreasing; q is transformed displacement variable.

IDENTIFICATION AND OPTIMAL OF PARAMETERS

Using the differential Eq.(9) of displacement transformation variables divided by the differential of deformation of member in relation to time, the Eq.(9) can be substituted by the following expression:

$$q' = \frac{dq}{dx} = \alpha - \eta \left(\beta \cdot \text{sign}(\dot{x}) |q|^{n-1} q + \gamma |q|^n \right) \tag{11}$$

The discrete form of Eq.(11) is:

$$\Delta q_i = [\alpha - \eta_i \left(\beta \cdot \text{sign}(\dot{x}_i) |q_i|^{n-1} q_i + \gamma |q_i|^n \right)] \Delta x_i \tag{12}$$

The three variables are defined as follows:

$$y_{1i} = \Delta x_i \tag{13a}$$

$$y_{2i} = \left(\eta_i \cdot \text{sign}(\dot{x}_i) |q_i|^{n-1} q_i \right) \Delta x_i \tag{13b}$$

$$y_{3i} = \left(\eta_i |q_i|^n \right) \Delta x_i \tag{13c}$$

Then, the Eq.(13) can be arranged as follows:

$$\Delta q_i = \alpha y_{1i} - \beta y_{2i} - \gamma y_{3i} \tag{14}$$

Thus, Δq_i is the linear function of y_{1i} , y_{2i} , y_{3i} and the

optimal coefficients of α , β and γ can be acquired by the fitting method of least squares. The method is discussed as follows: When the displacement increases gradually, the experimental data Δx_i are needed in Eq.(13) for calculating variables y_{1i} , y_{2i} , y_{3i} . Using R_i , restitution force for each time step to substitute into the related hysteretic restitution force equation to calculate the q_i value at each step, the transformed displacement variable with the restitution force is defined as follows:

$$q_i = \frac{R_i - \nu K_0 x_i}{(1 - \nu) K_0} \quad (15)$$

Where: ν is stiffness rate before and after yielding; x_i is system displacement for each time step; K_0 and ν can be estimated in accordance with the test data or converged to a very good result after several iteration steps. As to η_i of Eqs.(13b) and (13c), the assumed hardening coefficient μ substitutes into x_i and the yielding displacement of Δy_i is judged by Eq.(6) at that step and substituted into Eq.(10) to acquire η . Thereupon, substitute x_i , q_i , and η_i into Eqs.(13a)–(13c) to obtain y_{1i} , y_{2i} , y_{3i} at each step. Applying the fitting method of least square, the q_0 must be defined as a constant value that is always set to be zero; then the following simultaneous equations should be solved.

$$\begin{bmatrix} \sum y_{1i}^2 & -\sum y_{1i}y_{2i} & -\sum y_{1i}y_{3i} \\ \sum y_{2i}^2 & \sum y_{2i}y_{3i} & \\ \text{sym.} & \sum y_{3i}^2 & \end{bmatrix} \begin{Bmatrix} \alpha \\ \beta \\ \gamma \end{Bmatrix} = \begin{Bmatrix} \sum y_{1i}\Delta q_i \\ -\sum y_{2i}\Delta q_i \\ -\sum y_{3i}\Delta q_i \end{Bmatrix} \quad (16)$$

The optimal parameters α , β and γ , based on the proposed analytical model, can be acquired by the Eq.(16).

VERIFICATION OF NUMERICAL MODEL

The application of the proposed mathematical model, based on Wen’s model, was tested and verified by the actual test data. The test results, using displacement increasing under reciprocating loading test, were fitted based on the mathematical model proposed in this paper. The optimal parameters were calculated by the method of Statistics. The error square root of fitting was used for fixed quantity and the standard deviation was used for each test result to discuss the suitability of the modified model. The fitting curves, shown in Figs.12 and 13, were obtained by substituting the optimal parameters, acquired from the displacement increasing under reciprocating loading test, into the modified Wen Model. The figures indicated the compatibility of the experimental data with the numerical simulation data of the modified Wen’s model.

CONCLUSION

Experimental results indicated that the newly developed energy absorber using the mechanical characteristics of LYS could increase the structure’s ductility and energy dissipation capability and thus

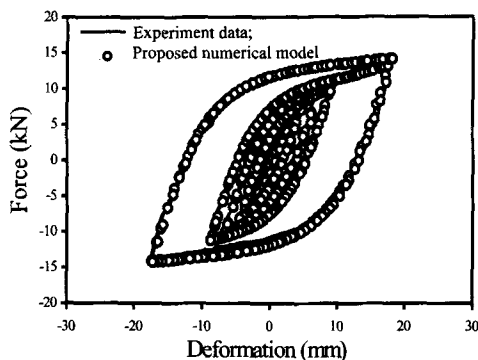


Fig.12 The fitting curve of experimental data and proposed numerical model for LYS-case 1

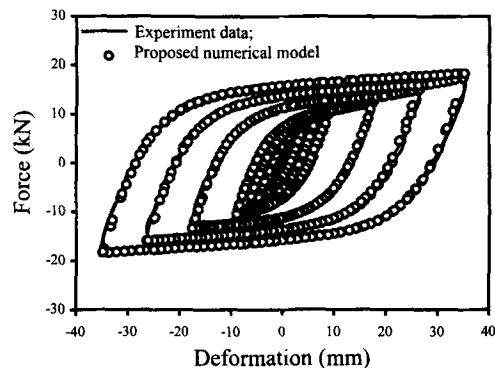


Fig.13 The fitting curve of experimental data and proposed numerical model for LYS-case 2

decrease the structure's reaction to earthquake. There are several advantages of this rhombic seismic resistance device. They are discussed as follows:

1. The rate of strain hardening of LYS is actually higher than that of A36 steel; and the yielding stress of LYS is just half that of A36 steel. The ultimate elongation of LYS is more than that of A36 steel by up to 60%.

2. The hysteresis loop of the experimental results indicated that the rhombic steel plate has outstanding qualifications and stable energy dissipation capability. Poor quality welding cannot adversely influence the energy absorber, and the manufacturing cost of this device can be lowered.

3. The good mechanical property of strain hardening of LYS steel can be used to lessen local fracture problem at the steel plate energy dissipator; and can also attain the energy dissipation design requirement of the same transformations of curvature, and make the total yielding on steel plate uniform and thus, increase the effect of energy dissipation.

4. Comparison of experimental and numerical data showed that the proposed mathematical model can correctly describe the hysteretic behavior of this device under reciprocating loading test.

In brief, this newly developed added damping and stiffness with LYS steel proposed in this paper, is very useful and worthy of expanded application for seismic resistance of structure. The proposed analytical model can be actually applied for improving the energy dissipation behavior of LYS-ADAS.

ACKNOWLEDGEMENT

The China Steel Corporation Company support of this work is gratefully acknowledged. The authors would also like to thank the editors of JZUS and English consultant Dr. Wong and anonymous referees for their careful reading of the paper and several suggestions, which have helped to improve the paper.

References

- Bouc, R., 1967. Forced Vibration of Mechanical System with Hysteresis. *In: Proceedings of the 4th International Conference on Nonlinear Oscillations*. Prague, Czechoslovakia.
- Chang, J.T., Wang, S.C., 1997. The Development of Ultra Low Yield Strength Plate Shell. China Steel Technical Report, 11.
- Constantinou, M.C., Soong, T.T., Dargush, G.F., 1998. Passive Energy Dissipative Systems for Structural Design and Retrofit. *In: Multidisciplinary Center for Earthquake Engineering Research, A National Center of Excellence in Advanced Technology Applications*. University at Buffalo, U.S.A.
- Gere, J.M., Timoshenko, S.P., 1990. *Mechanics of Materials*, 3rd Edition. PWS-KENT.
- Iwata, M., Huang, Y.H., Kawai, H., Wada, A., 1995. Study on damage tolerant structures. *Journal of Technology and Design-A.I.J.*, (1):82-89.
- Mendelson, A., 1970. *Plasticity: Theory and Application*.
- Tanaka, K., Sasaki, Y., 2000. Hysteretic Performance of Shear Panel Dampers of Ultra Low-Yield-Strength Steel for Seismic Response Control of Buildings. 12th World Conference on Earthquake Engineering, WCEE. New Zealand.
- Tsai, K.C., 1992. Steel Triangular Plate Energy Absorber for Earthquake-Resistant Buildings. *Proceedings, the First World Conference on Constructional Steel Design*. Acapulco, Mexico.
- Tsai, K.C., Li, C.W., Hong, C.P., Chen, H.W., Su, Y.F., 1993. Welded Steel Triangular Plate Device for Seismic Energy Dissipation. *Proceedings, ATC-17-1 Seminar on Seismic Isolation, Passive Energy Dissipation and Active Control*.
- Tsai, C.S., Le, H.H., 1993. Applications of viscoelastic dampers to high-rise buildings. *Journal of Structural Engineering, ASCE*, 119(4):1222-1233.
- Tsai, K.C., Chou, C.C., 1996. Plasticity models and seismic performance of steel plate energy dissipators. *Journal of the Chinese Institute of Civil and Hydraulic Engineering*, 8(1):45-54.
- Wada, A., Connor, J.J., Kawai, H., 1992. Damage Tolerant Structures. *In: Fifth US-Japan Workshop on the Improvement of Building Structural Design and Construction Practices*. ACT-15:1-13.
- Wen, Y.K. 1976. Method for random vibration of hysteretic systems. *Journal of Engineering Mechanics, ASCE*, 102(2):249-263.
- Whittaker, A., Bertero, V.V., Alonso, J., 1989. Earthquake simulator testing of steel plate added damping and stiffness elements. *In: Report No. 89/02, Earthquake Engineering Research Center*. University of California, Berkeley, CA, U.S.A.
- Xia, C., Hanson, R.D., 1992. Influence of ADAS element parameters on building seismic response. *Journal of Structural Engineering, ASCE*, 118(7):1903-1918.